RSC Advances

ROYAL SOCIETY OF CHEMISTRY

www.rsc.org/advances

Cure kinetics and physical properties of poly(dicyclopentadiene/5-ethylidene-2-norbornene) initiated by different Grubbs' catalysts

Guang Yang[a], Timothy C. Mauldin[b], Jong Keun Lee[a]*

[a]Department of Polymer Science and Engineering, Kumoh National Institute of Technology
Gumi, 730-701, Republic of Korea

[b]IBM Corporation, Materials Engineering, Tucson, AZ 85744, USA

Abstract: Cure kinetics of *endo*-dicyclopentadiene (DCPD)/5-ethylidene-2-norbornene (ENB) blends with the 1st and 2nd generation Grubbs' catalysts were characterized using dynamic differential scanning calorimetry. The results of the analysis revealed that the reactions with both Grubbs' catalysts were greatly accelerated by adding ENB. However, a strong dependence was observed on the fractional conversion and the type of catalyst used. The addition of ENB and different Grubbs' catalysts was found to have significant effects on gel fraction and crosslinking density of the resulting polymers. Although the modulus and maximum stress of the resulting polymers were observed to decrease slightly, tensile tests showed that the yielding strain and tensile toughness were enhanced with ENB loading. The glass transition temperature and thermal stability of the polymers with both catalysts decreased with increasing ENB loading. The effects of the different Grubbs' catalysts on cure kinetics and various physical properties are discussed in detail.

Keywords: *endo*-dicyclopentadiene, 5-ethylidene-2-norbornene, Grubbs' catalyst, ring-opening metathesis polymerization

1. Introduction

Thermoset polymers based on the ring-opening metathesis polymerization (ROMP) of *endo*-dicyclopentadiene (DCPD) to form poly(dicyclopentadiene) (polyDCPD) have attracted much attention as a matrix material due to their ease of fabrication, low material cost, processability, and the potential for post-polymerization modification of the preserved olefins along the main chain.[1] A combination of favorable physical and chemical properties,[2] i.e., high modulus, excellent impact strength, and chemical resistance, has resulted in an impetus for widespread use in various fields.[3]

To extend the potential use of polyDCPD in a variety of fields, attempts have been made to improve the performance of DCPD by blending with 5-ethylidene-2-norbornene (ENB).[4-9] The ENB monomer is known to be much more reactive in the presence of a low catalyst loading than DCPD in ROMP and has a very low melting point of -80 °C.[4, 10] Therefore, DCPD can be blended with ENB to provide a more reactive system to save production cost, thereby making it to be more suitable for practical use. Also, DCPD/ENB blends in the presence of Grubbs' catalyst as self-healing candidates have been investigated in our laboratory.[5-7] The DCPD/ENB blends do not have a significant melting point down to -40 °C, and the cure process is accelerated after adding ENB, even after substantial reductions in the amount of catalyst. Dynamic mechanical analysis showed that the DCPD/ENB blend in the ratio of 1:3 by weight has the highest storage modulus (after an isothermal cure time of 120 min) relative to other blending ratios.[5] Hence, ENB-rich blends have good potential as self-healing agents owing to enhanced cure kinetics at both a wider temperature range and a much lower catalyst level. Incorporation of ENB monomer is a useful approach to tune properties of polyDCPD blends, as the

* *Corresponding author. Tel.: +82-54-4787686; Fax: +82-54-4787710*
E-mail address: jklee@kumoh.ac.kr

glass transition temperature (T_g) of fully cured blends decreases linearly from ~160 °C (for neat polyDCPD) to ~120 °C (for neat polyENB), and a single T_g of blends implies the formation of random copolymer networks.[6] In addition, DCPD-rich monomer blends lead to improved adhesive bond strengths to epoxy substrates, with maximum bond strengths achievable at DCPD:ENB=3:1 at all cure conditions studied.[7] Blends of DCPD/ENB were also studied by other researchers. Kessler et al.[4, 8] investigated the ROMP kinetics of a DCPD/ENB mixture by evaluating the effect of cure on the viscosity and found that the ENB-containing blends are able to accelerate both initiation rate and cure rate after initiation, in comparison with neat DCPD. Additionally, several different variables—i.e., test temperature, catalyst concentration, and catalyst morphology—have significant influence on the polymerization initiation and propagation rates of the blend. In another unique application of ENB/DCPD blends, Ban[9] noted that when DCPD is copolymerized with ENB in an emulsion-type polymerization, the resulting latexes were more resistant to coagulation and flocculation, relative to neat polyDCPD colloids.

(a)

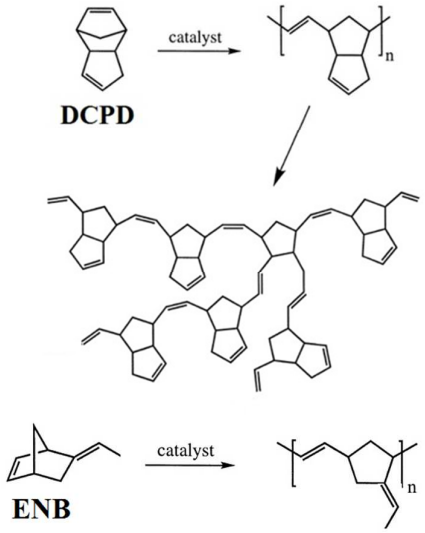

(b)

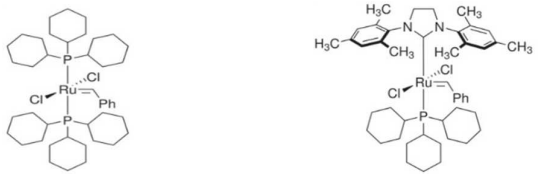

1st generation 2nd generation

Fig. 1. (a) ROMP schemes of DCPD and ENB and (b) chemical structures of the 1st and 2nd generation Grubbs' catalysts

As a result of the substantial difference in the reactivity of DCPD's two olefins, resulting in part from different ring strain energy between the strained norbornene and cyclopentene,[11] polymerization of neat DCPD is probably carried out in two steps (Fig. 1a): norbornene units of higher ring strain energy open first without much accompanying reaction of the cyclopentene units, resulting in the formation of a linear structure, followed by subsequent reaction of the cyclopentene rings to form a

crosslinked network.[12, 13] On the other hand, only linear molecules are formed by the ROMP of the strained norbornene olefin in ENB (Fig. 1a). Hence, the copolymerization of DCPD and ENB monomers is likely beset with a variety of intricate reaction sequences and functional group interactions, yet understanding the copolymerization mechanism of what is becoming known as an immensely useful comonomer blend can aid in optimizing these materials towards desirable properties. In other words, because of differential catalyst activity and selectivity, the backbone architecture of resulting DCPD/ENB polymers are complex, and physical and chemical properties of materials with various permutations of catalyst and comonomer types and loadings may differ substantially. In this study, we investigated the cure kinetics and thermo-mechanical properties of DCPD/ENB blends with two kinds of Grubbs' catalysts: the 1st and 2nd generation (Fig. 1b). The cure kinetics of DCPD/ENB blends was determined by dynamic differential scanning calorimetry (DSC) according to the model-free isoconversional method in order to elucidate the reaction mechanism. The cured blends were characterized by measuring gel fraction and estimating crosslinking density. In addition, the mechanical properties and thermal stability of the resulting polymers were analyzed using a universal testing machine (UTM), dynamic mechanical analysis (DMA) and thermogravimetric analysis (TGA).

2. Experimental

2.1. Materials

Endo-dicyclopentadiene (DCPD, 95%, Acros Organics, Belgium) and 5-ethylidene-2-norbornene (ENB, 99%, Sigma Aldrich, USA) were used as received without further purification. The 1st and 2nd generation Grubbs' catalysts (Sigma Aldrich, USA) were recrystallized to allow better dissolution kinetics based on a literature procedure.[14] Toluene was purchased from Dae Jung, Korea and also used as received to evaluate the swelling behavior of the prepared polymer.

2.2. Preparation of uncured samples and DSC measurements

Five different loadings of ENB (0, 12.5, 25, 37.5 and 50 wt%) were added to DCPD and stirred for 10 min until a homogeneous solution was obtained. Then the resulting solution was cooled to 15 °C and the recrystallized 1st or 2nd Grubbs' catalyst was quickly dissolved (i.e., <30 s) in the solution *via* vigorous stirring to yield a homogenous reaction mixture. Finally, the mixture was immediately placed in liquid nitrogen to prevent undesired cure reaction prior to use. To avoid excessively fast cure or incomplete cure caused by inadequate catalyst amount, the fixed catalyst amount of 2.0 mg/mL was used in this work.[5, 6] Exotherms of the dynamic reactions as a function of temperature for all DCPD/ENB samples were performed using a DSC (200 F3 Maia, Netzsch, Germany). Approximately 10 mg of the frozen solution was enclosed in an aluminum DSC pan and immediately subjected to a heating run from -50 to 250 °C at heating rates of 5, 10, 15, and 20 °C/min under a constant nitrogen flow.

2.3. Fabrication of cured samples

Homogeneous solutions of DCPD/ENB blends with the 1st or 2nd generation Grubbs' catalyst were prepared as described above. Polymer samples were prepared by injecting the reaction mixture into a brass mold covered with ParaFilm (Bemis, USA), and successively cured for 24 h at 25 °C, for 2 h at 70 °C, and for 1.5 h at 170 °C. Upon completion, the polymer samples were cooled to room temperature and removed from the mold. To diminish the influence of surface oxidation,[15] the samples were polished with abrasive papers one day after sample preparation.

2.4. Gel fraction and swelling measurements

Soxhlet extraction of polymer samples was carried out to determine gel fraction. Typically, a previously cured specimen (~100 mg) was placed into a cellulose thimble and refluxed using a toluene/ethyl vinyl ether solvent (5:1 by weight) for 48 h. Ethyl vinyl ether was used to quench any active catalyst remaining in the materials from inducing undesirable metatheses reactions. After extraction, the solvent contained in the insoluble component was evaporated in a vacuum oven at 70 °C overnight. The gel fraction was calculated using the following equation,

$$\text{Gel fraction (\%)} = \frac{W_2}{W_1} \times 100\% \quad (1)$$

where W_1 is the initial weight and W_2 is the weight of the insoluble portion.

For the fully gelled samples with no weight loss after extraction in the solvent, swelling tests were performed to estimate the extent of crosslinking. Samples were immersed in a toluene/ethyl vinyl ether solvent (5:1 by weight) at room temperature for 48 h to reach the absorption equilibrium. The swollen specimens were then removed and weighed (W_s). Subsequently, the absorbed solvent was evaporated by drying the specimens overnight in a vacuum oven at 70 °C, and the weight of the deswollen specimens (W_{ds}) was determined. The swelling ratio is defined in Eq. (2) below,

$$\text{Swelling ratio (\%)} = \frac{W_s - W_{ds}}{W_{ds}} \times 100\% \quad (2)$$

2.5. Tensile tests and SEM observation

Tensile properties of various cured DCPD/ENB blends, i.e., elastic modulus, tensile strength, and strain at break, were determined with a UTM (AG-50KNX, Shimadzu, Japan). The series of tests were carried out as per an ASTM standard D638-V method at a crosshead speed of 1 mm/min at room temperature. The average values of more than five tests were reported in this study. The morphology of fracture surfaces after tensile tests was observed by field-emission scanning electron microscopy (FE-SEM, JSM-6500F, Jeol, Japan).

2.6. Dynamic mechanical analysis

DMA was performed using a TA Instruments DMA Q800. The cured specimens [35 mm (L) × 12 mm (W) × 3 mm (T)] were analyzed at a constant frequency of 1 Hz and a heating rate of 2 °C/min from room temperature to 200 °C in the dual cantilever mode. Storage modulus (E') and tan δ values as a function of temperature were obtained for all cured samples under identical conditions. The T_g corresponds to a temperature at which the tan δ value reaches a peak.

2.7. Thermogravimetric analysis

TGA of the cured blends were measured using a TA Instruments model Q500 TGA at a heating rate of 20 °C/min from room temperature to 600 °C under nitrogen atmosphere. A small amount of cured polymer (~6 mg) was used for the TGA measurement. The weight loss and decomposition rate as a function of temperature were recorded.

3. Results and discussion

3.1. Thermochemical analysis

3.1.1. Dynamic cure of DCPD/ENB blends

Dynamic DSC measurements were performed at different heating rates of 5, 10, 15, and 20 °C/min for DCPD blended with 0, 12.5, 25, 37.5, and 50 wt% of ENB monomer using the 1st and 2nd generation Grubbs' catalysts. Fig. 2 shows typical dynamic DSC traces for various DCPD/ENB reaction systems with the 1st and 2nd generation Grubbs' catalysts at the same heating rate of 10 °C/min. Obvious differences in heat flow are observed between the 1st and 2nd generation Grubbs' catalyst systems. In the 1st generation catalyst system (Fig. 2a), the DSC curve of pure DCPD shows a single exothermic peak maximum at ~90 °C. When 12.5 wt% of ENB is added to DCPD, a shoulder appears in the lower temperature range of ~10–30 °C. It is clear that the shoulder at lower temperature is due to the reaction of the added ENB. With an increase in the ENB content above 25 wt%, the shoulder at the lower temperature is converted into a peak maximum at ~40 °C, while the peak at higher temperature (75–150 °C) becomes a weaker shoulder. Sheng et al.[16] have reported the cure process of ENB and *endo*-DCPD with the 1st generation Grubbs' catalyst using a dynamic DSC technique at a heating rate of 10 °C/min and observed an apparent distinction in the location of their exothermic peaks, concluding that the ROMP reaction of the ENB monomer occurs earlier than that of the DCPD monomer. Therefore, such changes in the DSC curves for the blends with different ENB loadings are probably the result of the asynchronous polymerization of ENB and DCPD monomers.

As seen in the 2nd generation catalyst system (Fig. 2b), each of the DSC curves, irrespective of the ENB loading, exhibits a comparable and sharp exothermic peak with a shoulder in the range of 60–150 °C. The inset in the Fig. shows a shoulder for the blend DCPD/ENB = 50/50, although this is typically observed in all blends with this catalyst. The shoulders at the end of the cure process of the 2nd generation catalyst system may be the result of the cross metathesis reactions between linear double bonds produced by the ROMP reactions of norbornene and cyclopentene rings. Since the ROMP processes produce a new metal-alkylidene complex, they are generally followed by the cross metathesis reactions.[17, 18] However, the ROMP and subsequent cross metathesis strongly depend on the type of Grubbs' catalyst. According to Grubbs' early work.[19, 20] the cross metathesis reactions are known to be more prominent in the systems with the 2nd generation Grubbs' catalyst than those with the 1st generation catalyst system. Furthermore, unlike the 1st generation catalyst system, no significant reaction separation is observed for all DCPD/ENB blends with the 2nd generation Grubbs' catalyst, which suggests that the ROMP reaction of the two monomers occurs simultaneously in the presence of the 2nd generation Grubbs' catalyst. The simultaneous ROMP reactions of DCPD and ENB in the presence of the 2nd generation Grubbs' catalyst may lead to different molecular structures compared to the 1st generation Grubbs' catalyst as will be discussed later.

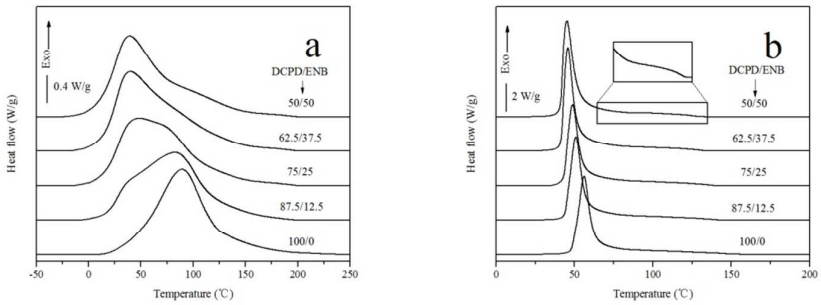

Fig. 2. Typical DSC thermograms of DCPD/ENB blends with (a) the 1st generation and (b) the 2nd generation Grubbs' catalysts at a heating rate of 10 °C/min.

Table 1 lists the onset cure temperature (T_{onset}), peak temperature (T_p), and total enthalpy of reaction (ΔH_R) from integration of the exothermic peak shown in Fig. 2 for each blend at a heating rate of 10 °C/min. As the ENB loading increases in both catalyst systems, the exothermic peaks, i.e., T_{onset} and T_p, shift gradually to lower temperatures, which is attributed to the much faster ROMP reactivity of the ENB monomer than that of the DCPD monomer [5, 6]. Meanwhile, the total enthalpy (ΔH_R) increases with an increase of ENB level, which suggests that the ROMP reaction of the ENB monomer is more exothermic. In addition, the 2nd generation catalyst system has a higher T_{onset} and ΔH_R, relative to the 1st generation catalyst system, but a lower T_p. These findings, to some extent, support that the reaction mechanism of the system may be dependent on the type of the catalysts used.

Table 1. Onset and peak cure temperatures, T_{onset} and T_p, and total enthalpy, ΔH_R, for different cure systems at a heating rate of 10 °C/min.

	DCPD/ENB (wt%)	T_{onset} (°C)	T_p (°C)	ΔH_R (J/g)
1st generation catalyst	100/0	6.8	88.9	445.2
	87.5/12.5	–3.5	81.3	461.3
	75/25	–13.7	47.2	483.3
	62.5/37.5	–20.8	39.6	493.9
	50/50	–26.4	39.0	502.0
2nd generation catalyst	100/0	34.4	56.2	456.0
	87.5/12.5	27.8	50.9	463.2
	75/25	23.2	48.9	483.2
	62.5/37.5	15.3	45.8	496.1
	50/50	14.1	45.2	507.1

3.1.2. Isoconversional kinetic analysis

As discussed in the above section, although some helpful information about the dynamic cure reaction of DCPD/ENB blends has been obtained, it is still insufficient to account for the complex reaction mechanism. In this regard, isoconversional kinetic analysis, assuming that the reaction rate at a certain conversion is merely a function of the temperature, can give us a more direct and deeper insight into complicated cure processes. Through this analysis, the dependence of activation energy (E_α) on fractional conversion (α) for the entire cure reaction is determined, which can be correlated to a variety of reaction mechanisms during the cure process of DCPD/ENB blends with different Grubbs' catalysts. Among the numerous isoconversional computation methods, the advanced isoconversional method developed by Vyazovkin[21-23] exhibits an unparalleled accuracy and extensive applicability. In the Vyazovkin method, the E_α value at a particular conversion can be determined by minimizing the following equation:

$$\Phi(E_\alpha) = \sum_{i=1}^{n} \sum_{j \neq i}^{n} \frac{J[E_\alpha, T_i(t_\alpha)]}{J[E_\alpha, T_j(t_\alpha)]}$$

$$J[E_\alpha, T_i(t_\alpha)] \equiv \int_{t_{\alpha-\Delta\alpha}}^{t_\alpha} exp[\frac{-E_\alpha}{RT_i(t)}] \quad (3)$$

where the subscripts i and j denote thermal measurements at different heating rates, $\Delta\alpha$ is the increment of conversion ($\Delta\alpha$ = 0.025 in this work), and t_α and $t_{\alpha-\Delta\alpha}$ are the cure times up to

fractional conversions α and $\alpha - \Delta\alpha$, respectively. Minimization is repeated for each conversion to produce a dependence of E_α on the conversion α.

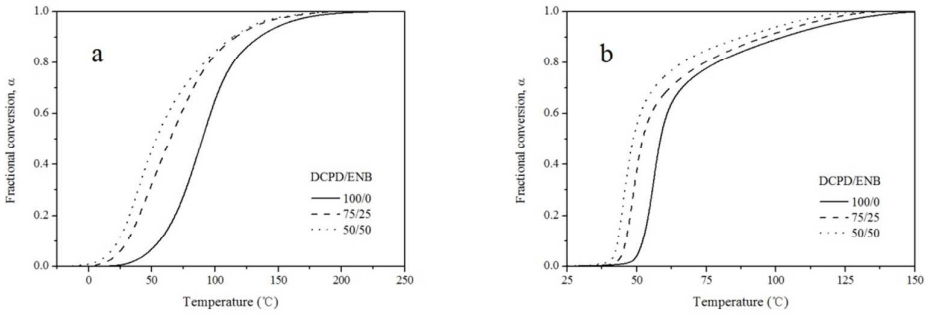

Fig. 4. Fractional conversion versus temperature for DCPD/ENB blends with (a) the 1st generation and (b) the 2nd generation Grubbs' catalysts.

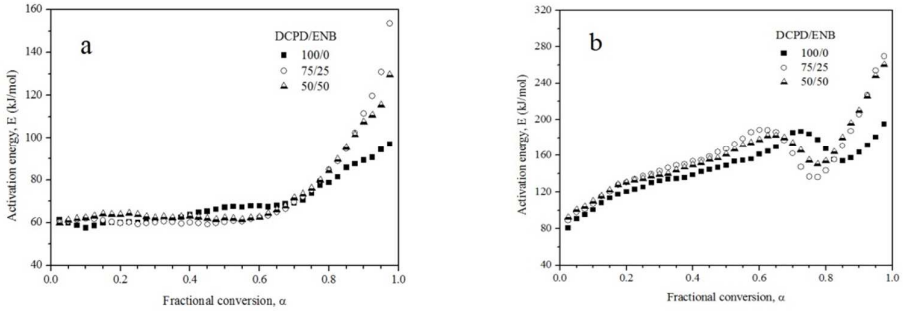

Fig. 5. Activation energy as a function of the fractional conversion for DCPD/ENB blends with (a) the 1st generation and (b) the 2nd generation Grubbs' catalysts.

In order to determine the effect of ENB loading and Grubbs' catalyst on the reaction mechanism, typical samples containing 0, 25, and 50 wt% ENB loadings with the 1st and 2nd generation Grubbs' catalysts were selected to be investigated in the following sections. Fig. 4 displays the relationship between fractional conversion and cure temperature for different DCPD/ENB reaction systems with the 1st and 2nd generation Grubbs' catalysts. As ENB loading increases, the temperature at a fractional conversion value decreases in both catalyst systems. The comparison of the two Fig.s also definitely exhibits that the 2nd generation catalyst enables the reaction of the blend system to be completed in a smaller temperature range relative to the 1st generation catalyst.

According to the correlation between conversion and temperature as shown in Fig. 4, the dependence of activation energy (E_α) on the fraction conversion (α) for different reaction systems was obtained using Eq. (3), as illustrated in Fig. 5. Note that E_α depends strongly on α for both the Grubbs' catalyst systems, which could reflect changing reaction mechanisms during each stage of the cure process. The difference in E_α-α correlation for the 1st and 2nd generation catalyst systems also implies noticeable differences in the reaction mechanisms are associated with the type of the catalyst used. These findings reveal that the dynamic cure reactions of DCPD/ENB blends with the 1st and 2nd generation catalysts are multiple kinetic processes. Nevertheless, for α < ~0.6, the effect of ENB loading on the E_α value has no apparent effect on the observed E_α-α relationships for all DCPD/ENB

blends in each catalyst system. This observation potentially indicates that the norbornene olefin in DCPD and ENB monomers has an identical reaction mechanism under the respective Grubbs' catalysts, thus the E_α-α relationship of the blend systems maintains an analogous shape and values in this region irrespective of the addition of ENB. As seen in Fig. 5a, all samples initiated with the 1st generation catalyst show a similar trend with α. At the beginning of the cure process with the 1st generation catalyst system, E_α remains nearly constant at ~60 kJ/mol up to $\alpha \approx 0.6$, above which E_α rapidly increases as α continues to increase. The norbornene olefin of DCPD and ENB monomers, because of relief of its higher ring strain upon opening relative to that of the cyclopentene olefin, is known to exhibit a higher reactivity and undergoes ROMP first, which is likely responsible for the constant activation energy. After a particular conversion is reached ($\alpha \approx 0.6$), the less reactive cyclopentene rings participate in the reaction, which contributes to the increased activation energy. Moreover, the addition of ENB component leads to an increased fraction of norbornene units, and thus the reaction of cyclopentene rings, occurring after the ROMP of norbornene rings, likely requires more energy to allow catalyst to penetrate the higher viscosity network resulting from the prior polymerization of the higher fraction of norbornene units. As a consequence, higher activation energy for DCPD/ENB blends is observed at the end of the cure process, relative to the activation energy of neat polyDCPD formation at high conversions.

The variation of E_α versus α for the DCPD/ENB blends initiated by the 2nd generation Grubbs' catalyst is more complicated (Fig. 5b). The different blends in the 2nd generation catalyst system also show a tendency for higher values in E_α during the entire cure process in comparison with the 1st generation catalyst system. Evidently, at the initial stage of the reaction for the 2nd generation catalyst system, E_α of different mixtures increases with increasing conversion until α of ~0.2. This corresponds to the induction period for reaction system, during which time polymerization is minimal. Following this initiation period, the norbornene and cyclopentene rings undergo polymerization simultaneously, owing to a greater affinity of the 2nd generation catalyst to both norbornene and cyclopentene olefins relative to the 1st generation catalyst, although the ring-opening of norbornene olefins is still dominant during this phase.[24] This unique reactivity is accompanied by an increase in viscosity of the reaction mixture that is not as prominent as with the 1st generation catalyst, owing to the 2nd generation catalyst's concurrent cyclopentene ring-opening leading to hyperbranching intermediate structures at lower conversions. These factors are responsible for restricted diffusion of the unreacted groups, thereby leading to an increase in E_α in the range of $\alpha \approx 0.2–0.7$. When the conversion further increases, an unexpected drop in E_α is noted for all reaction blends. This observation is similar to the previous results from the dynamic reaction of DCPD-Grubbs' catalyst system.[25] The drop corresponds to the shoulder observed in DSC scans and thus can be considered as a sign of the cross metathesis reactions of the linear olefins that can be more prominent in the 2nd generation catalyst system.[19, 20] In comparison with the unreacted cyclic olefins restricted by the increased viscosity, the linear olefins are omnipresent throughout the entire network, which leads to that the cross metathesis reactions become dominant relative to the ROMP. The effect of the cross metathesis on E_α also becomes more prominent, and the ease of cross metathesis thus leads to the decrease in E_α. Moreover, the drop in E_α shifts towards lower conversion after adding ENB, which implies that ENB can catalyze the cross metathesis process that is unique to the 2nd generation Grubbs' catalyst. At the end of the cure process, the DCPD/ENB blends in 2nd generation catalyst system also exhibit higher E_α than pure DCPD, which can be explained in the same manner as with the 1st generation catalyst system at high conversions.

3.2. Gel fraction and swelling measurements

The swelling behavior of DCPD/ENB polymers was evaluated in terms of gel fraction and swelling ratio. Gel fraction and swelling ratio values of the entire chemical network were determined from the equilibrium solvent swelling method for cured DCPD/ENB specimens. Fig. 6 shows the gel fraction and swelling ratio of different blends with various ENB loadings. PolyDCPD, initiated by the 1st or 2nd generation catalyst, shows no weight loss, which indicates the formation of a completely gelled structure. With the addition of ENB, the gel fraction of DCPD/ENB blends maintain 100% weight in the 1st generation catalyst system, whereas its gel weight steadily decreases in the 2nd generation catalyst system and only 4 wt% of the gel content remains in the cured specimens when the ENB loading increases up to 50 wt%. This phenomenon is associated with the reaction mechanisms of different catalyst systems. In the 1st generation catalyst system, norbornene rings open from the onset of the cure process to form linear chains. When linear chains are near fully developed, the subsequent reaction of less reactive cyclopentene units is more effective to construct a crosslinked network due to the lower activation energy and fewer viscosity limitations discussed above. Nevertheless, following an initiation period, both olefin types in the 2nd generation catalyst system simultaneously undergo reaction to form complex branching structures, resulting in rapid viscosity increases and hence diffusion-based limitations to forming substantial crosslinks.

In order to qualitatively estimate chemical crosslinking density, swelling tests were conducted on completely gelled samples: all samples with the 1st generation catalyst and pure polyDCPD with the 2nd generation catalyst. Swelling ratio for the cured specimens with the 1st generation catalyst slightly increases with ENB loading, which implies that the chemical crosslinking density of the blends decreases with the increase of ENB loading. The decrease in chemical crosslinking density can be attributed to the formation of only a linear structure by polymerization of ENB monomers, which leads to an increase of molecular weight between crosslinks. However, the comparison in swelling ratio between the 1st and 2nd generation catalyst systems shows that the 1st generation catalyst samples have a much higher chemical crosslinking density, while the 2nd generation catalyst is less effective in the production of crosslinks. Such enormous variations in gel fraction and swelling ratio between the two catalyst systems reveal the difference in the chemical structure of two types of cured samples produced with different catalysts.

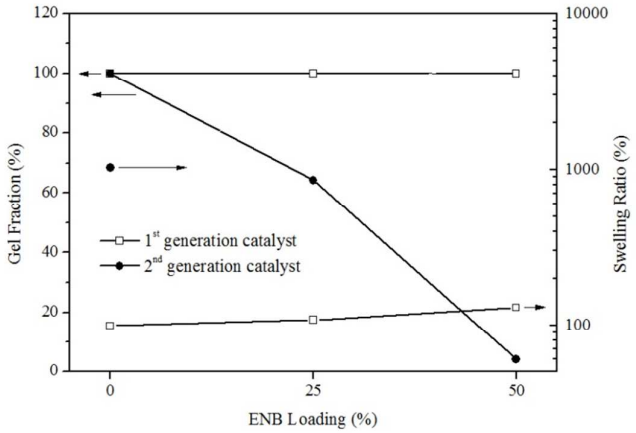

Fig. 6. Gel fraction and swelling ratio of cured DCPD/ENB blends with the 1st and 2nd generation Grubbs' catalysts.

3.3. Tensile properties

Fig. 7 shows representative stress–strain curves of cured DCPD/ENB blends with different ENB loadings and Grubbs' catalysts. All cured samples show a typical plastic deformation behavior. When a sample is stretched to its ultimate tensile strength, yield occurs; then, the sample necks with a local decrease in width within the gauge region. As the sample extends further, the necking zone propagates along the gauge region until the sample fractures.

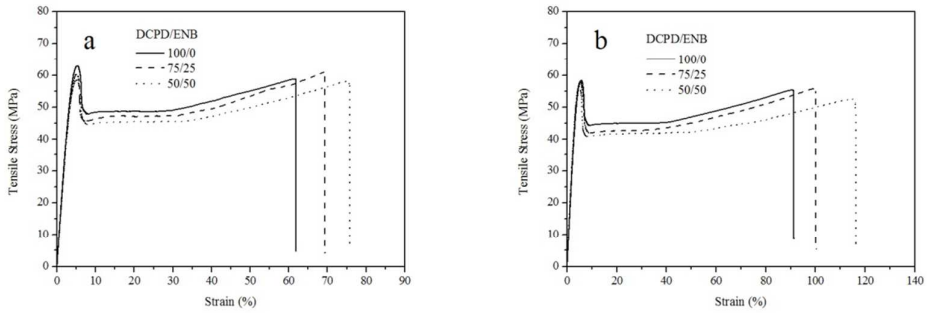

Fig. 7. Stress–strain curves of cured DCPD/ENB blends with (a) the 1st generation and (b) the 2nd generation Grubbs' catalysts.

Table 2. Summary of tensile test results for cured DCPD/ENB blends.

	DCPD/ENB	E (GPa)	σ (MPa)	ε (%)	Toughness (MPa)
1st generation catalyst	100/0	1.82±0.04	62.89±0.85	61.87±4.08	31.39±4.36
	75/25	1.78±0.04	60.78±1.02	69.14±1.57	34.71±3.46
	50/50	1.72±0.02	58.51±1.28	75.82±2.56	36.68±3.48
2nd generation catalyst	100/0	1.75±0.03	58.42±0.78	91.36±7.64	43.35±6.85
	75/25	1.71±0.05	57.87±0.46	100.20±6.56	46.55±5.23
	50/50	1.67±0.02	56.60±0.77	116.22±8.16	51.88±7.17

The Young's modulus (E), yield tensile stress (σ), strain at break (ε) and tensile toughness calculated from the total area under stress-strain curve of cured DCPD/ENB blends are listed in Table 2. It is evident that the tensile properties are dependent on ENB loading and type of catalysts. In comparison with those with the 2nd generation catalyst, the samples with the 1st generation catalyst show relatively higher E and σ, but lower ε and tensile toughness. These are likely caused by the configuration of the polymeric backbone (e.g., *trans* vs. *cis*) and the crosslinking density. Many investigations have previously been done on the stereospecific nature of polyDCPD produced by the 1st and 2nd generation Grubbs' catalysts.[26, 27] The significant difference in the configuration of the polymeric backbone was identified; a predominant *trans* double bond configuration for the 1st generation Grubbs' catalyst and a poor stereoselectivity for the 2nd generation Grubbs' catalyst. For thermosetting networks, it is well known that the modulus and tensile stress are primarily proportional to the packing density of the glassy state.[28] The 1st generation catalyst system, mainly consisting of *trans* polymer, is confirmed to pack more efficiently and thus be more rigid, while the 2nd generation catalyst system, containing both the *trans* and the *cis* configuration, is more malleable. On the other hand, the relatively lower crosslinking density in the 2nd generation catalyst system increases the free

volume of chain segments, thereby improving the movement of polymer chains in different directions.[29] The increased mobility of chain segments results in a reduced packing and lower modulus of network. Moreover, in both catalyst systems, E and σ of cured samples moderately decrease with ENB loading, which is associated with the decreased crosslinking density. Upon incorporation of 50 wt% ENB loading, the ε value given in Table 2 significantly increases from 61.9% to 75.9 % for the 1st generation catalyst system and from 91.4% to 116.2% for the 2nd generation catalyst system. The linear molecular chain formation during the polymerization of ENB, which extends the molecular weight between crosslinks, may result in the promotion of slippage among polymeric chains. Notice that the tensile toughness of the blends increases by 5.29 MPa and 8.53 MPa for the 1st and 2nd generation catalyst systems, respectively, with addition of 50 wt% ENB, which can also be attributed to the inability of ENB in producing crosslinks.

The fracture surface of tensile blends using the 1st and 2nd generation catalysts was observed by scanning electron microscopy, as shown in Fig. 8. The morphology of DCPD/ENB blends becomes relatively rougher with ENB loading in both catalyst systems, which is a sign of the increase in toughness. Moreover, the specimens initiated with the 2nd generation catalyst exhibit higher surface area morphologies in comparison with those using the 1st generation catalyst, which analogously indicates that the samples using the 2nd generation catalyst have increased toughness over those made with the 1st generation catalyst.

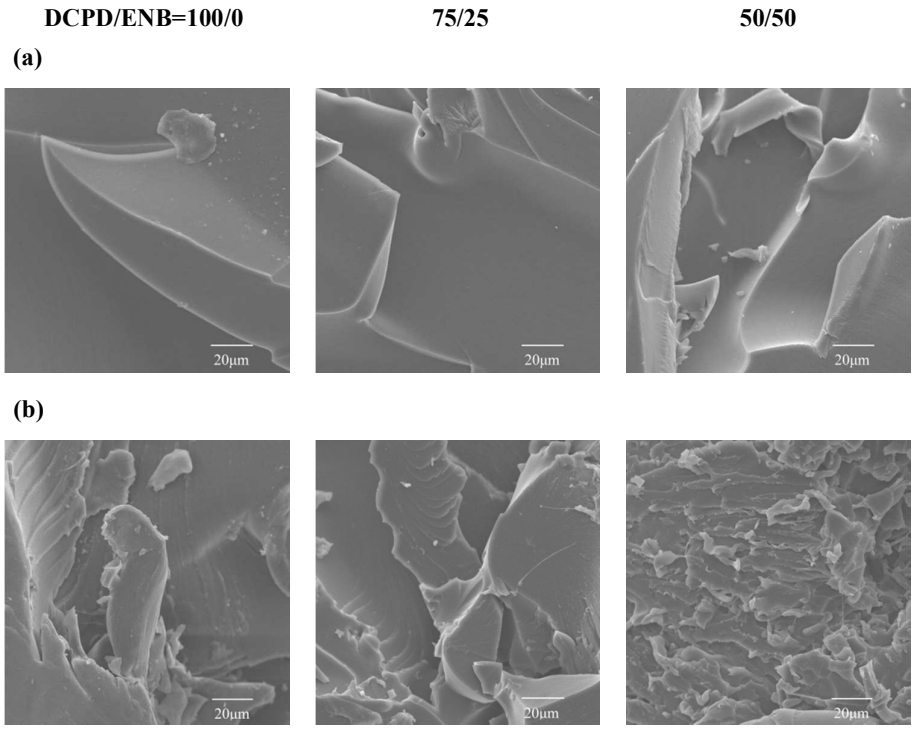

Fig. 8. SEM images of the fracture surface of tensile specimens with (a) the 1st generation and (b) the 2nd generation Grubbs' catalysts.

3.4. Thermo-mechanical properties

DMA was performed in order to evaluate the effect of ENB loading and catalyst type on the thermal and viscoelastic properties of the DCPD/ENB blends. In this work, T_g was determined from the

peak of the tan δ curve. From the rubber elasticity theory, the crosslinking density (v_e) can be calculated through the storage modulus in the rubbery plateau at 30 °C above T_g using the following equation:

$$E' = 3v_eRT \quad (4)$$

where E' is the storage modulus in the rubbery plateau region above T_g (T_g + 30°C), R is the gas constant, and T is the absolute temperature corresponding to E' (K).

Storage modulus and mechanical loss factor of cured specimens as a function of temperature are shown in Fig. 9. The calculated v_e and the results obtained from DMA tests are listed in Table 3. As expected from the tensile tests, the storage modulus in the glassy state (at 30 °C) only decreases slightly with increasing ENB loading for both catalyst systems and each of the blends initiated with the 2nd generation catalyst has a lower storage modulus. The decrease in the storage modulus can be explained with the same reasons as described in the tensile tests.

As ENB loading increases in DCPD/ENB blends, T_g moves to lower temperatures (from 150.2 to 136.6 °C and from 150.8 to 131.3°C for the 1st and 2nd generation catalyst systems, respectively) and the tan δ peak height increases. This T_g phenomenon is associated with the crosslinking density. In general, the T_g of blends is strongly influenced by the crosslinking density. With addition of ENB, the formation of a few chemically crosslinked structures and the decrease of crosslinking density provide more free volume for chain segments to relax and heighten the chain motions, thus requiring lower temperatures or lesser energy for the onset of the glass transition. The specimens with higher ENB loading also show considerably higher tan δ peak height values, because the linear structure of the ENB polymer leads to an increase in molecular weight between crosslinks, which causes the improved flexibility of the network. The mixing rule for T_g of binary miscible DCPD/ENB blends can be described by the Fox equation:

$$\frac{1}{T_g} = \frac{w_1}{T_{g1}} + \frac{w_2}{T_{g2}} \quad (5)$$

where T_{g1} and T_{g2} represent the glass transitions, and w_1 *and* w_2 are the mass fractions of cured DCPD and ENB, respectively. The T_g of poly-ENB initiated by the 1st and 2nd generation catalysts was measured as 112.9 °C and 116.3 °C, respectively.[30] As shown in Table 3, the calculated T_g values of blends in the 1st generation catalyst system are 3.8 and 5.9 °C lower than the experimental values, whereas the calculated results in the 2nd generation catalyst system match very closely with the experimental values. DCPD and ENB monomers can polymerize into the crosslinked and linear structures, respectively; therefore, the Fox equation assumes the network structure as a binary blend of linear chains and crosslinks. However, from the swelling tests, it is clear that the 1st generation catalyst system has a completely crosslinked structure, irrespective of ENB loading, but the gel fraction in the 2nd generation catalyst system gradually decreases with increasing ENB loading. In other words, for the 1st generation catalyst system, the expected polymer network is different from the actual network, which explains the difference between experimental and calculated T_g values.

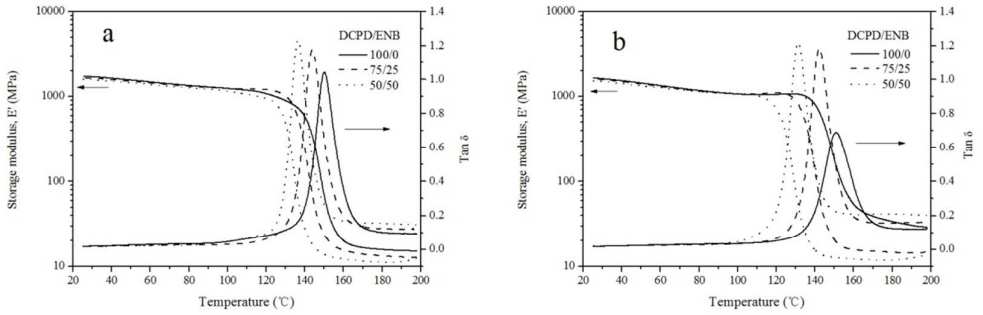

Fig. 9. Storage modulus (E') and loss factor (tan δ) as a function of temperature for the cured blends with (a) the 1st generation and (b) the 2nd generation Grubbs' catalysts.

When the sample is brought into a rubbery plateau above T_g, the storage modulus at T_g + 30 °C decreases with ENB loading for each catalyst system because of internal crosslinking density, which is supported by the calculated v_e using Eq. (4) as shown in Table 3. Storage modulus at T_g + 30 °C of the cured blends with the 1st generation catalyst is lower than those with the 2nd generation catalyst. It is also found that the v_e calculated using Eq. (4) reveals a trend opposite of that determined by the swelling experiments for the 1st and 2nd generation catalyst systems, although the trend is the same when varying the ENB loading within each catalyst system. This phenomenon is likely caused by the following factor. The sum of true-type chemical crosslinks as well as physical entanglements was determined in the case of dynamic mechanical analysis,[31, 32] whereas only the true chemical crosslinks were determined in the swelling experiments. Sheng[33] reported that an apparent crosslinking density can be calculated by Eq. (4) when ENB monomers polymerized into a polymer with a linear network, thereby concluding that physical crosslinks still contribute to the storage modulus in a rubbery state. The 2nd generation catalyst has a much higher ROMP reactivity than the 1st generation catalyst, which indicates that the entire cure process occurred in a very short period and greatly enhances the probability for the formation of entanglements. This fact is likely responsible for what initially appears to be conflicting results in crosslinking density trends derived from different methods.

Table 3. Summary of DMA results for DCPD/ENB blends.

	DCPD/ENB	T_g (°C)		E' at 30 °C	E' at T_g + 30 °C	v_e
		Exp.	Cal.	(MPa)	(MPa)	(mol/m^3)
1st generation catalyst	100/0	150.2	—	1698	15.69	1387
	75/25	144.0	140.2	1632	13.63	1222
	50/50	136.6	130.7	1571	11.71	1068
2nd generation catalyst	100/0	150.8	—	1608	33.58	2966
	75/25	142.3	141.6	1569	14.88	1339
	50/50	131.3	132.8	1484	12.16	1122

3.5. Thermogravimetric analysis

The comparative thermal stability of the cured blends initiated by the 1st and 2nd generation catalysts was evaluated by TGA with a heating rate of 20 °C/min under a N_2 atmosphere. The TGA thermographs for the weight and derivative-weight percentage as a function of temperature for the

cured blends are presented in Fig. 10. The characteristic degradation temperature, i.e. 5% degradation temperature ($T_{5\%}$), and the temperature at which maximum degradation rate occurs (T_{max}), are given in Table 4. All of the polymers exhibit a similar degradation feature. The cured blends were thermally stable up to 200 °C and slight degradation occurred between 200 and 400 °C, suggesting that the cured blends have sufficiently good thermal stability. Subsequently, the remainder of the cured blends degraded rapidly in the range of 400~500 °C, corresponding to the degradation of the bulk polymer. Nevertheless, the position of the 5% weight loss shifts to the lower temperature with the addition of ENB, i.e., from 447.7 to 408.4 °C for the 1st generation catalyst system and from 442.9 to 380.2 °C for the 2nd generation catalyst system with 50 wt% ENB loading. Thermal stability is also diminished in samples prepared using the 2nd generation catalyst system, relative to the 1st generation catalyst system. The decline of thermal stability for the cured blends is associated with the decreased crosslinking density. Furthermore, there are double peaks on all damping curves of blends with the 2nd generation catalyst (see the inset in Fig. 10b), whereas the 1st generation catalyst system only shows a single peak. These findings reveal the different network structures between the two kinds of catalyst systems and to some extent, also corroborate the different reaction mechanisms that are strongly dependent on the type of Grubbs' catalysts used.

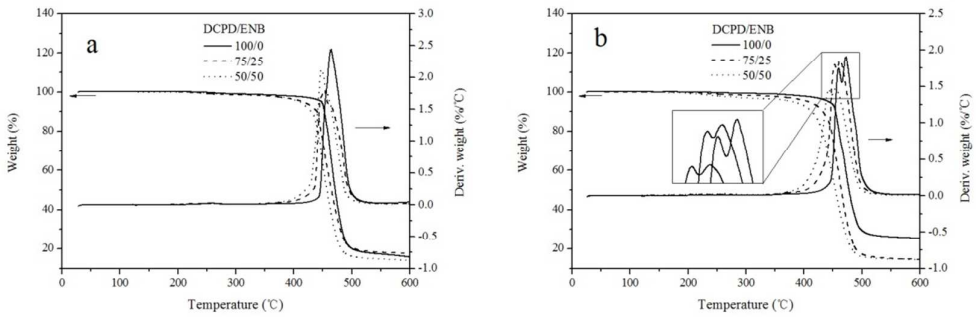

Fig. 10. TGA thermographs of the cured blends with (a) the 1st generation and (b) the 2nd generation Grubbs' catalysts.

Table 4. Thermogravimetric results for the cured blends

	DCPD/ENB	$T_{5\%}$ (°C)	T_{max} (°C)	
1st generation catalyst	100/0	447.7	464.3	
	75/25	415.0	452.8	
	50/50	408.4	448.2	
2nd generation catalyst	100/0	442.9	459.9	472.6
	75/25	407.5	453.2	462.5
	50/50	380.2	442.7	454.8

4. Conclusions

The influence of ENB loading and Grubbs' catalyst type on cure kinetics and physical properties of polyDCPD was studied. The polymerization of DCPD/ENB monomers initiated by various catalysts shows different reaction dynamics. DSC curves of the 1st generation catalyst system become asymmetric after adding ENB, because of the asynchronous conversion of DCPD and ENB monomers,

whereas those of the 2nd generation catalyst system exhibit a comparable exothermic peak with a shoulder. Addition of ENB and the 2nd generation catalyst can significantly accelerate the cure process of DCPD, which shifts the reaction to a lower temperature and a shorter time. Activation energy (E_α) for all specimens as a function of fraction conversion (α) indicates that the cure process of DCPD/ENB blends with the 1st and 2nd generation catalysts results from complex combinations of multiple reactions occurring at different stages in the curing cycles. The gel fraction and swelling behavior of the cured specimens imply that crosslinking is suppressed by addition of ENB and when using the 2nd generation catalyst. This decreased crosslinking density due to ENB loading and the 2nd generation catalyst acts to improve strain at break and toughness, albeit accompanied by a slight modulus and yield stress decrease. The glass transition temperature (T_g), strongly coupled to the crosslinking density, also shifts towards a lower temperature with ENB loading. In the rubbery state, the storage modulus of the 2nd generation catalyst system, although with a lower chemical crosslink density, is greater than that of the 1st generation catalyst system. This phenomenon is likely associated with physical crosslinks resulting from the much faster reaction of the 2nd generation catalyst system. Although the initial thermal decomposition temperature of the polymer networks decreases gradually as ENB loading increases, all polymers have good thermal stability up to ~400 °C.

Acknowledgement

This research was supported by Basic Science Research Program through the National Research Foundation of Korea (NRF) funded by the Ministry of Education, Science and Technology (NRF 2011-0009150).

References

1. M. Perring, T. R. Long and N. B. Bowden, *J. Mater. Chem.*, 2010, **20**, 8679-8685.
2. Kirk-Othmer, *Encyclopedia of chemical technology*, Wiley-Interscience, New York, 1996.
3. *US Pat.,* 6 020 443, 2000.
4. M. Kessler, G. Larin and N. Bernklau, *J. Therm. Anal. Calorim.*, 2006, **85**, 7-12.
5. X. Liu, J. K. Lee, S. H. Yoon and M. R. Kessler, *J. Appl. Polym. Sci.*, 2006, **101**, 1266-1272.
6. J. K. Lee, X. Liu, S. H. Yoon and M. R. Kessler, *J. Polym. Sci., Part B: Polym. Phys.*, 2007, **45**, 1771-1780.
7. G. C. Huang, J. K. Lee and M. R. Kessler, *Macromol. Mater. Eng.*, 2011, **296**, 965-972.
8. G. Larin, N. Bernklau, M. Kessler and J. DiCesare, *Polym Eng Sci*, 2006, **46**, 1804-1811.
9. H. T. Ban, M. Shigeta, T. Nagamune and M. Uejima, *J. Polym. Sci. Polym. Chem.*, 2013, **51**, 4584-4591.
10. A. Muhlebach, P. Van Der Schaaf, A. Hafner, R. Kolly, F. Rime and H. Kimer, in *Nato Science Series, Kluwer Academic Publishers*, 2002, pp. 23-44.
11. P. R. Khoury, J. D. Goddard and W. Tam, *Tetrahedron*, 2004, **60**, 8103-8112.
12. A. Bell, in *ACS Symp. Ser.*, American Chemical Society, Washington, DC, 1992, vol. 496, p. 308.
13. R. A. Fisher and R. H. Grubbs, *Makromolekulare Chemie. Macromolecular Symposia*, 1992, **63**, 271-277.
14. W. Jeong and M. Kessler, *Chem. Mater.*, 2008, **20**, 7060-7068.
15. D. R. Kelsey, H. H. Chuah, R. H. Ellison, D. L. Handlin and B. M. Scardino, *J. Polym. Sci. Polym. Chem.*, 1997, **35**, 3049-3063.

16. X. Sheng, M. Kessler and J. Lee, *J. Therm. Anal. Calorim.*, 2007, **89**, 459-464.
17. D. S. La, E. S. Sattely, J. G. Ford, R. R. Schrock and A. H. Hoveyda, *J. Am. Chem. Soc.*, 2001, **123**, 7767-7778.
18. T. L. Choi, C. W. Lee, A. K. Chatterjee and R. H. Grubbs, *J. Am. Chem. Soc.*, 2001, **123**, 10417-10418.
19. A. K. Chatterjee and R. H. Grubbs, *Org. Lett.*, 1999, **1**, 1751-1753.
20. T. L. Choi, A. K. Chatterjee and R. H. Grubbs, *Angew. Chem. Int. Edit.*, 2001, **40**, 1277-1279.
21. S. Vyazovkin and D. Dollimore, *J. Chem. Inf. Comput. Sci.*, 1996, **36**, 42-45.
22. S. Vyazovkin, *J. Comput. Chem.*, 1997, **18**, 393-402.
23. S. Vyazovkin, *J. Comput. Chem.*, 2001, **22**, 178-183.
24. G. O. Wilson, M. M. Caruso, N. T. Reimer, S. R. White, N. R. Sottos and J. S. Moore, *Chem. Mater.*, 2008, **20**, 3288-3297.
25. G. Yang and J. K. Lee, *Thermochim. Acta*, 2013, **566**, 105-111.
26. A. Bang, D. Mohite, A. M. Saeed, N. Leventis and C. Sotiriou-Leventis, *J. Sol-Gel Sci. Techn.*, 2015, **75**, 1-15.
27. D. Schaubroeck, S. Brughmans, C. Vercaemst, J. Schaubroeck and F. Verpoort, *J. Mol. Catal. A: Chem.*, 2006, **254**, 180-185.
28. E. F. Oleinik, *Adv. Polym. Sci.*, 1986, **80**, 49-99.
29. K. P. Menard, *Dynamic mechanical analysis: a practical introduction*, CRC press, 2008.
30. G. Yang and J. K. Lee, Unpublished results.
31. P. K. Maji and A. K. Bhowmick, *J. Polym. Sci. Polym. Chem.*, 2009, **47**, 731-745.
32. V. Sekkar, *J. Appl. Polym. Sci.*, 2010, **117**, 920-925.
33. X. Sheng, J. K. Lee and M. R. Kessler, *Polymer*, 2009, **50**, 1264-1269.